



Superconducting properties of single-crystalline $A_x\text{Fe}_{2-y}\text{Se}_2$ ($A=\text{Rb}, \text{K}$) studied using muon spin spectroscopy

Z. Shermadini,^{1,*} H. Luetkens,¹ R. Khasanov,¹ A. Krzton-Maziopa,² K. Conder,² E. Pomjakushina,² H.-H. Klauss,³ and A. Amato¹

¹Laboratory for Muon Spin Spectroscopy, Paul Scherrer Institute, CH-5232 Villigen PSI, Switzerland

²Laboratory for Developments and Methods, Paul Scherrer Institute, CH-5232 Villigen PSI, Switzerland

³Institut für Festkörperphysik, TU Dresden, D-01069 Dresden, Germany

(Received 22 November 2011; revised manuscript received 23 December 2011; published 5 March 2012)

We report on the superconducting properties of $A_x\text{Fe}_{2-y}\text{Se}_2$ ($A=\text{Rb}, \text{K}$) single crystals studied with the muon spin relaxation or rotation (μSR) technique. At low temperatures, close to 90% of the sample volumes exhibit large-moment magnetic order which impedes the investigation of their superconducting properties by μSR . On the other hand, about 10% of the sample volumes remain paramagnetic and clearly show a superconducting response. The temperature dependence of the superconducting carrier density was analyzed within the framework of a single s -wave gap scenario. The zero-temperature values of the in-plane magnetic penetration depths $\lambda_{ab}(0) = 258(2)$ and $225(2)$ nm and the superconducting gaps $\Delta(0) = 7.7(2)$ and $6.3(2)$ meV have been determined for $A = \text{Rb}$ and K , respectively. The microscopic coexistence and/or phase separation of superconductivity and magnetism is discussed.

DOI: [10.1103/PhysRevB.85.100501](https://doi.org/10.1103/PhysRevB.85.100501)

PACS number(s): 74.70.Xa, 76.75.+i, 74.25.Ha

The recent discovery of superconductivity in iron selenide compounds $A_x\text{Fe}_{2-y}\text{Se}_2$ and $(\text{Ti}, A)_x\text{Fe}_{2-y}\text{Se}_2$ (where $A = \text{K}, \text{Rb}, \text{Cs}$),^{1–4} with transition temperatures up to about 32 K, has led to a renewed interest in iron-based chalcogenide systems. The average crystal structure of these materials is of the ThCr_2Si_2 type (space group $I4/mmm$).⁵ A remarkable observation is that, besides the superconducting state, a strong antiferromagnetic state with magnetic moments up to $3.3 \mu_B$ per Fe ion are observed below $T_N = 478$ K, 534 K, and 559 K for $A = \text{Cs}, \text{Rb}$, and K , respectively (see Refs. 6–9). Actually, the stoichiometry of the parent compound appears to be near $\text{A}_{0.8}\text{Fe}_{1.6}\text{Se}_2$ (hence the often used denomination “245”). Fe vacancy order has been found to occur below a structural phase transition T_S taking place well above T_N .^{7,9,10}

As the interplay with magnetism is thought to play a major role in understanding the properties of the superconducting state in iron-based systems, many studies have been devoted to this topic. The coexistence of magnetism and superconductivity has been reported in pnictide-“122” systems.^{11–13} A characteristic of this iron-based family is that the temperature of the magnetic transition needs to decrease by doping or external pressure prior to observing a superconducting state at low temperature. Hence, it appears that in the pnictide-122 systems static magnetism has to be destroyed by a control parameter such as doping or pressure before superconductivity can develop its full strength.^{14,15} On the other hand, there are some indications that the interplay in the chalcogenide iron-based systems might be rather opposite in nature than the one observed in the pnictides. Hence, an unusual behavior has been reported in the FeSe_{1-x} family under pressure, where one observes that both the magnetic¹⁶ and superconducting^{16,17} transition temperatures increase with increasing pressure above 0.8 GPa.

Hence, as a new iron-based chalcogenide superconductor family, the $A_x\text{Fe}_{2-y}\text{Se}_2$ systems have attracted many studies focused on the understanding of the nature of the interplay between the strong magnetic state occurring at high temperature

and the superconductivity in the same samples. Muon spin relaxation or rotation (μSR),⁸ transport and magnetization,⁶ specific heat, magneto-optical imaging,¹⁸ and Mössbauer¹⁹ spectroscopy suggest a microscopic coexistence and the bulk character of both the strong antiferromagnetism and superconductivity. Some studies claim that superconductivity only occurs in the compositions when Fe content is compatible with a vacancy order pattern; the ground state of the material becomes metallic and superconductivity sets in.²⁰ Alternatively, others suggest that superconductivity is achieved when the Fe vacancies are disordered and that superconductivity and magnetism occur in the same samples, but microscopically separated.²¹ In this Rapid Communication, we report on μSR studies specifically devoted to superconducting properties of the $A_x\text{Fe}_{2-y}\text{Se}_2$ systems, shedding more light on the question of the bulk character of the superconducting state at low temperatures.

Single crystals were grown from a melt using the Bridgman method.³ The homogeneity and elemental composition of cleaved crystals have been studied using x-ray fluorescence spectroscopy (XRF; Orbis Micro-XRF Analyzer, EDAX), and were characterized by powder x-ray diffraction using a D8 Advance Bruker AXS diffractometer with $\text{Cu K}\alpha$ radiation. The final compositions were found to be $\text{Rb}_{0.77}\text{Fe}_{1.61}\text{Se}_2$ and $\text{K}_{0.74}\text{Fe}_{1.66}\text{Se}_2$. Magnetization and resistivity measurements have been performed with a physical property measurement system Quantum Design 9T.

For the μSR measurements, performed using the transverse-field (TF) and zero-field (ZF) techniques, the DOLLY instrument located on the $\pi E1$ beam line of the Swiss Muon Source (Paul Scherrer Institute, Villigen, Switzerland) was used. Measurements were performed using a static helium flow cryostat between 2 and 40 K.

A first step of our study has been to elucidate the superconducting properties of the $A_x\text{Fe}_{2-y}\text{Se}_2$ crystals by performing in-plane zero-field-cooling (ZFC) magnetization measurements, shown in Fig. 1(a). Both samples exhibit sharp

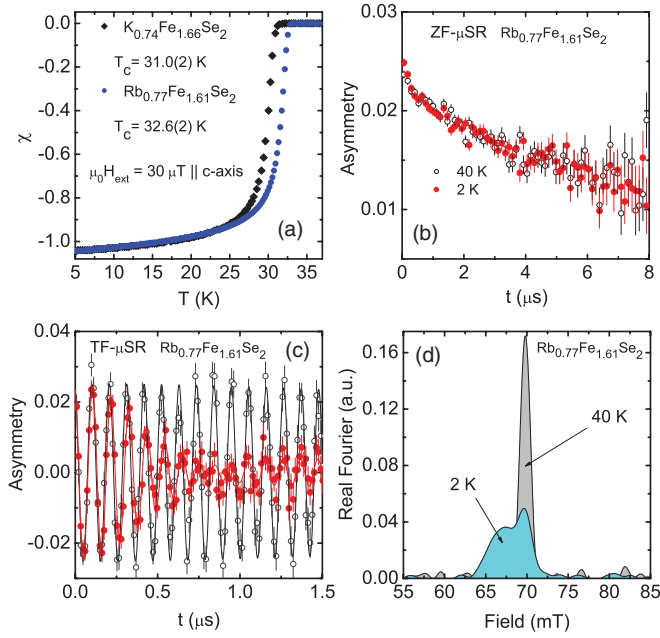


FIG. 1. (Color online) (a) Temperature dependence of the dc magnetic susceptibility obtained in a zero-field-cooling (ZFC) procedure. The data were obtained with an external magnetic field of $\mu_0 H_{\text{ext}} = 30 \mu\text{T}$ applied along the c axis. (b) Zero-field (ZF) and (c) transverse-field (TF) μSR time spectra recorded above and below T_c . The TF data have been obtained with an external field of 0.07 T and in a field-cooling procedure. (d) Fourier transform of the TF μSR spectra shown in panel (c).

superconducting transitions at $T_c = 31.0(2)$ K and $32.6(2)$ K for $A = \text{K}$ and Rb , respectively, and a nearly 100% Meissner screening is observed. The respective T_c values are compatible with the ones extracted by resistivity (not shown). However, as will be discussed below, the magnetization study alone is necessary but not sufficient to claim a 100% superconducting volume fraction,²² even though it is very often used that way.

The first goal of our μSR study was to check the magnetic properties by the ZF and weak TF (wTF) technique. In agreement with our previous measurements,⁸ we observe that a large fraction of the μSR signal is wiped out at very early time (i.e., $t \ll 0.1 \mu\text{s}$), in the wTF as well as in the ZF measurements, due to a large internal field and/or a broad field distribution in the antiferromagnetic phase of the sample.²³ From the wTF measurements it is derived that this phase represents about 88% and 89% of the sample volume for $A = \text{Rb}$ and K , respectively. The rest of the signal represents a fraction of the sample remaining in a paramagnetic state below T_N . This sample fraction is characterized by a weak muon depolarization which is found to be constant between 40 K and 2 K [see for example the case of $A = \text{Rb}$ in Fig. 1(b)]. This temperature independence of the ZF relaxation indicates that 12% (11%) of the Rb (K) sample volume is free of a magnetic transition at least down to 2 K.

This fraction of the sample remaining paramagnetic below T_N opens the possibility to study the superconducting state by μSR , using the μSR TF technique.²⁴ The first step of our TF μSR measurements was to determine the optimal external magnetic field H_{ext} (with $H_{\text{ext}} > H_{c1}$) for which a maximal

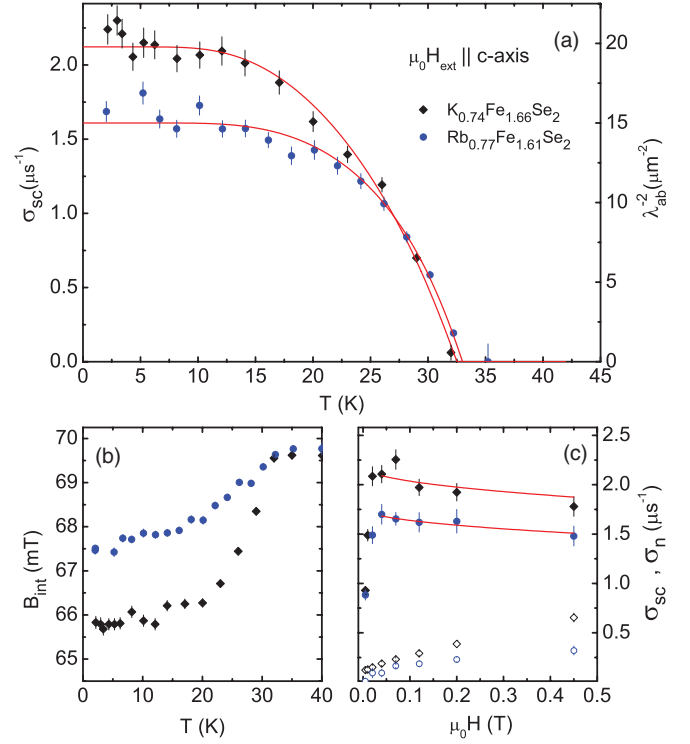


FIG. 2. (Color online) (a) Temperature dependence of $\sigma_{\text{sc}} \sim \lambda_{\text{ab}}^{-2}$ and therefore of the superfluid density n_s [see Eq. (2) and text] measured in an applied field of $\mu_0 H_{\text{ext}} = 0.07$ T. (b) Temperature dependence of the internal field B_{int} sensed by the muons. (c) Field dependence of the muon depolarization rate above (40 K; open symbols) and below (2 K; closed symbols) T_c . The external field was applied along the crystallographic c axis.

muon spin depolarization rate (σ_{sc} , see below) occurs due to the buildup of a flux line lattice (FLL) in the mixed state of the superconductor.²⁵ The field dependence of σ_{sc} was obtained upon field cooling from above T_c down to 2 K for each data point [see Fig. 2(c)]. For both Rb and K systems, the optimum field is above 0.07 T and a complete temperature scan was performed with this external field applied along the c axis. Typical μSR spectra, as well as the corresponding Fourier transforms, are reported in the panels (c) and (d) of Fig. 1 for $A = \text{Rb}$.

The TF- μSR time spectra were analyzed using a two-Gaussian depolarization function:

$$A_0 P(t) = A_{\text{sc}} \exp\left(-\frac{(\sigma_{\text{sc}}^2 + \sigma_{\text{n}}^2)t^2}{2}\right) \cos(\gamma_{\mu} B_{\text{int}} t + \varphi) + A_{\text{bg}} \exp\left(-\frac{\sigma_{\text{bg}}^2 t^2}{2}\right) \cos(\gamma_{\mu} B_{\text{bg}} t + \varphi), \quad (1)$$

where A_{sc} is an initial asymmetry, B_{int} represents the internal magnetic field at the muon site, and σ_{sc} is the Gaussian relaxation rate reflecting the second moment of the magnetic field distribution due to the FLL in the mixed state. σ_{n} , representing the depolarization due to the nuclear magnetic moments, is taken from the fits above T_c and considered as temperature independent down to 2 K. The second term of Eq. (1) represents a background signal (bg) corresponding to

muons stopping in the cryostat walls; A_{bg} , σ_{bg} , and B_{bg} denote the initial asymmetry (about 18% of A_0), the relaxation rate, and magnetic field (which has essentially the value of the external field) sensed by muons stopped in the background.

Due to the very high damping signal occurring in the antiferromagnetic phase of the sample⁸ one is unable to measure any superconducting response for this fraction. However, as discussed below, this does not exclude that such a phase presents also a superconducting state.

Figure 2(a) exhibits for both systems the temperature dependence of the muon depolarization rate σ_{sc} reflecting the field distribution created by the FLL. The temperature dependence of the average value of the internal field B_{int} sensed by the muon ensemble is reported in Fig. 2(b). A clear diamagnetic response of the samples is observed below T_c . Considering an extreme-type-II superconductor, one can evaluate the London magnetic penetration depth λ and superfluid density n_s from the second moment of the magnetic field distribution inside the sample in the mixed SC state, or alternatively, from the Gaussian muon spin depolarization rate σ_{sc} .²⁵

$$\frac{\sigma_{sc}^2(T)}{\gamma_\mu^2} = 0.00371 \frac{\Phi_0^2}{\lambda_{ab}^4(T)}, \quad (2)$$

where $\Phi_0 = 2.068 \times 10^{-15}$ Wb is the magnetic flux quantum, and $\gamma_\mu/2\pi = 135.5$ MHz T⁻¹ is the muon gyromagnetic ratio (note that as the external field is applied along the c axis; we are probing the penetration depth λ_{ab} in the basal plane). In turn, from the temperature dependence of λ_{ab} , one obtains the temperature evolution of the superfluid density n_s as $n_s(T)/n_s(0) = \lambda_{ab}^{-2}(T)/\lambda_{ab}^{-2}(0)$. Here we would like to mention that the described analysis neglects any additional contribution to the μ SR relaxation rate due to possible FLL disorder or induced magnetism.²⁶ Therefore the extracted value of the penetration depth represents a lower limit. The temperature dependence of n_s was analyzed within the framework of a BCS single s -wave symmetry superconducting gap Δ .^{27,28} The results of the analysis for $A_x\text{Fe}_{2-y}\text{Se}_2$ ($A = \text{K}, \text{Rb}$) are reported in Fig. 2(a). The solid line represents the fit of a simple s -wave model to the data. Due to the flattening of $\sigma_{sc}(T)$ below $T_c/2$ a clean d -wave model is incompatible with the data. Note that a two gap ($s + s$) as well as an anisotropic s -wave scenario provides also a satisfactory χ^2 fitting criteria. The parameters extracted from the fitting procedure using the simplest s -wave model are summarized in Table I. The observed values of $2\Delta(0)/k_B T_c$ indicate that $A_x\text{Fe}_{2-y}\text{Se}_2$ systems are in the strong-coupling limit.

The reader should keep in mind that the penetration depth obtained from the data analysis corresponds to the

TABLE I. List of the parameters obtained from the analysis of the temperature dependence of n_s .

	Rb _{0.77} Fe _{1.61} Se ₂	K _{0.74} Fe _{1.66} Se ₂	Unit
T_c	32.6(2)	31.0(2)	K
$\lambda_{ab}(0)$	258(2)	225(2)	nm
$\Delta(0)$	7.7(2)	6.3(2)	meV
$2\Delta(0)/k_B T_c$	5.5(2)	4.7(2)	

paramagnetic fraction representing about 12% of a total sample volume. We note that NMR measurements²⁹ gave $\lambda = 290$ nm, which is also almost certainly representative for the paramagnetic fraction only since the NMR signal from the strong antiferromagnetic regions of the sample is probably wiped out. On the other hand, macroscopic magnetization³⁰ and torque³¹ measurements give a considerably longer $\lambda = 580$ and 1800 nm, respectively, since they probably reflect a kind of average over the whole sample. Our analysis provides also a slightly lower value of the superconducting gap than the one measured by the ARPES technique³² (isotropic superconducting gap of 10.3 meV).

Figure 2(c) shows the field dependence at 2 K of the muon depolarization rate obtained upon field cooling from above T_c down to base temperature. Above $\mu_0 H_{ext} = 0.07$ T, σ_{sc} decreases only very slightly indicating a high value of the critical field H_{c2} . Previous measurements reported values on the order of $\mu_0 H_{c2}^c(0) = 60$ T for Rb_{0.88}Fe_{1.76}Se₂ (Ref. 4) and for K_{0.8}Fe_{1.81}Se₂ (Ref. 33). The solid lines in Fig. 2(c) correspond to a fit based on the numerical Ginzburg-Landau model (NGL) with the local (London) approximation ($\lambda \gg \xi$; ξ is the coherence length)²⁵ for both systems. This model describes the magnetic field dependence of the second moment of the field distribution created by the FLL and therefore the field dependence of the μ SR depolarization rate. Fixing the value of $\mu_0 H_{c2}(2 \text{ K}) = 55$ T found in the literature^{4,33} and considering λ_{ab} as a free parameter, we get $\lambda_{ab}(2 \text{ K}) = 246(1)$ and 221(3) nm for $A = \text{Rb}$ and K , respectively. These values are in good agreement with the values obtained by studying the temperature dependence of the muon depolarization rate (see Table I).

Since the observation of strong magnetism ($m_{Fe} > 2 \mu_B$ and $T_N = 478$ K)⁸ in one of the members of the newly discovered $A_x\text{Fe}_{2-y}\text{Se}_2$ superconductors, the most intriguing question to answer by theory as well as by experimental observation is whether or not superconductivity and magnetism may coexist microscopically or whether they live apart together in the same sample but in a phase-separated manner. Unfortunately experimental techniques that simultaneously can measure strong magnetism and superconductivity locally are lacking. Therefore conclusions have to be drawn from a combination of observations obtained from two or more experimental methods. There are good arguments for both scenarios. First we will summarize a few arguments in favor of bulk superconductivity.

In a first step we will discuss techniques that provide macroscopic information on the superconducting state. In the majority of the reports on the superconducting properties of the new compounds a 100% Meissner screening is observed by magnetization measurements, for a great variety of compounds (see, e.g., Ref. 6). Even a decent diamagnetic screening is sometimes observed in field-cooled magnetization experiments.³⁴ Also a sizable peak is observed in specific-heat measurements^{18,35,36} at the superconducting T_c . A superconducting volume fraction of 92–98% is estimated from the specific-heat data by comparing the zero-temperature residual and the normal-state Sommerfeld coefficients.³⁵ These two different macroscopic observations in favor of bulk superconductivity can anyhow be questioned. In samples showing a 100% Meissner response, anomalies in the magnetic

hysteresis loop were found that can be understood in the picture that superconductivity in the sample is percolative with weakly coupled superconducting islands.²² The interpretation of specific-heat data in view of the superconducting volume fraction is dangerous since it relies on the determination of the electronic Sommerfeld coefficient which is assumed to be the same for the whole sample. This assumption might anyhow not be valid for a potential phase separation into metallic and insulating volumes. Strong evidence for bulk superconductivity comes from magneto-optical imaging¹⁸ of a uniform flux distribution after the sample was cooled in a field which was switched off at low temperatures. This is consistent with the bulk superconducting nature of the sample and shows that it is not filamentary or phase separated.¹⁸ Further, different magnetization measurements yield a rather large $\mu_0 H_{c1} = 13$ mT and a corresponding magnetic penetration depth of $\lambda = 580$ nm³⁰ which is hard to understand for filamentary superconductivity. On the other hand, in the samples showing indications of bulk superconductivity, i.e., 100% Meissner screening, neutron scattering experiments observe a block spin antiferromagnetic ordering without traces of a secondary phase, suggesting a microscopic coexistence of magnetism and superconductivity.^{7,9,10} Another argument for a microscopic coexistence comes from two-magnon Raman scattering.³⁷ The intensity of the two-magnon peak which reflects directly magnetic order undergoes a clear, steplike reduction on entering the superconducting phase which suggests a microscopic coexistence of antiferromagnetic order and superconductivity. Recent inelastic neutron scattering studies³⁸ observed a magnetic resonant mode below T_c in the $\text{Rb}_2\text{Fe}_4\text{Se}_5$ system. Such observation also suggests that bulk SC coexists with $\sqrt{5} \times \sqrt{5}$ magnetic superstructure.

There are several experiments revealing different kinds of phase separation in different $A_x\text{Fe}_{2-y}\text{Se}_2$ compounds. Depending on the experimental technique they are able to directly detect a structural, nonsuperconducting/superconducting or a magnetic/nonmagnetic phase separation. The determination of a magnetic/superconducting phase separation by these techniques is anyhow only possible on the basis of plausible arguments. Transmission electron microscopy (TEM) reveals a rich variety of microstructures related to Fe vacancy order.³⁹ The superconducting samples clearly appear to be phase separated suggesting that the superconducting phase could have a Fe vacancy disordered state. Similarly, scanning nanofocus single-crystal x-ray diffraction⁴⁰ reveals a structural phase separation in domains with a compressed and an expanded lattice structure where the latter might be associated with a magnetic phase adopting a Fe vacancy ordered structure. On the contrary, scanning tunneling microscopy (STM) able to detect local structural and electronic properties indicates a

microscopic coexistence of superconductivity and a $\sqrt{2} \times \sqrt{2}$ charge modulation likely caused by block-spin antiferromagnetic ordering.⁴¹ It should be noted anyhow that the STM measurements did not observe the usually observed Fe vacancy ordering pattern (which according to neutron measurements exhibits a block-spin antiferromagnetic state) but rather a vacancy-free FeSe layer and therefore there might be as well two different magnetic structures.

Optical spectroscopy observes a Josephson-coupling plasmon of superconducting condensate.⁴² This together with a TEM analysis suggests a nanoscale stripe-type phase separation between superconductivity and insulating phases. In addition, optical conductivity measurements in the THz region observe a very low charge carrier density in favor of a phase-separated picture with a minor metallic and a dominant semiconducting phase.⁴³

Local probe techniques such as μSR (our present and earlier studies)⁸ and Mössbauer^{19,44,45} show a phase separation into a 85–95% major magnetic and a 15–5% minor nonmagnetic volume fraction. The paramagnetic fraction studied by μSR gives a typical response of superconducting character. Based on the experimental results one can suppose that (i) only the antiferromagnetic, (ii) only the paramagnetic, or (iii) both regions are superconducting. The experimental evidence reported here strongly excludes the first case. On the other hand, the second scenario is challenged by many experimental results mentioned above. Unfortunately, the μSR technique alone is unable to exclude the second and third scenarios because of a very high damped muon polarization signal coming from the large antiferromagnetic fraction. Since both scenarios have their own experimental support the question remains open and should trigger further studies of these systems.

In this study we showed that all our $A_x\text{Fe}_{2-y}\text{Se}_2$ samples exhibit a paramagnetic volume fraction of about 12%. The μSR signal of this fraction exhibits a rather weak ZF depolarization indicating that the paramagnetic islands are rather large, probably >100 nm. The superconducting response obtained by TF μSR is typical for a FLL of type-II superconductors again indicating paramagnetic grains larger than the distance of the flux lines. The temperature dependence of the superfluid density was described by a single s -wave gap model with zero-temperature values of the in-plane magnetic penetration depth $\lambda_{ab}(0) = 258(2)$ and $225(2)$ nm and superconducting gaps $\Delta(0) = 7.7(2)$ and $6.3(2)$ meV for $A = \text{Rb}$ and K , respectively.

The μSR experiments were performed at the Swiss Muon Source, Paul Scherrer Institut, Villigen, Switzerland. The authors thank the Sciex-NMSc^h (Project Code 10.048) and NCCR MaNEP for support of this study.

*zurab.sheradini@psi.ch

¹M. Fang, C. Wang, H. Dong, Z. Li, C. Feng, J. Chen, and H. Q. Yuan, *Europhys. Lett.* **94**, 27009 (2010).

²J. Guo, S. Jin, G. Wang, S. Wang, K. Zhu, T. Zhou, M. He, and X. Chen, *Phys. Rev. B* **82**, 180520 (2010).

³A. Krzton-Maziopa, Z. Shermadini, E. Pomjakushina, V. Pomjakushin, M. Bendele, A. Amato, R. Khasanov,

H. Luetkens, and K. Conder, *J. Phys. Condens. Matter* **23**, 052203 (2011).

⁴A. F. Wang, J. J. Ying, Y. J. Yan, R. H. Liu, X. G. Luo, Z. Y. Li, X. F. Wang, M. Zhang, G. J. Ye, P. Cheng *et al.*, *Phys. Rev. B* **83**, 060512 (2011).

⁵M. Rotter, M. Tegel, and D. Johrendt, *Phys. Rev. Lett.* **101**, 107006 (2008).

- ⁶R. H. Liu, X. G. Luo, M. Zhang, A. F. Wang, J. J. Ying, X. F. Wang, Y. J. Yan, Z. J. Xiang, P. Cheng, G. J. L. Z. Y. Ye *et al.*, *Europhys. Lett.* **94**, 27008 (2011).
- ⁷V. Y. Pomjakushin, E. V. Pomjakushina, A. Krzton-Maziopa, K. Conder, and Z. Shermadini, *J. Phys. Condens. Matter* **23**, 156003 (2011).
- ⁸Z. Shermadini, A. Krzton-Maziopa, M. Bendele, R. Khasanov, H. Luetkens, K. Conder, E. Pomjakushina, S. Weyeneth, V. Pomjakushin, O. Bossen *et al.*, *Phys. Rev. Lett.* **106**, 117602 (2011).
- ⁹B. Wei, H. Qing-Zhen, C. Gen-Fu, M. A. Green, W. Du-Ming, H. Jun-Bao, and Q. Yi-Ming, *Chin. Phys. Lett.* **28**, 086104 (2011).
- ¹⁰V. Y. Pomjakushin, D. V. Sheptyakov, E. V. Pomjakushina, A. Krzton-Maziopa, K. Conder, D. Chernyshov, V. Svitlyk, and Z. Shermadini, *Phys. Rev. B* **83**, 144410 (2011).
- ¹¹R. Khasanov, D. V. Evtushinsky, A. Amato, H.-H. Klauss, H. Luetkens, C. Niedermayer, B. Büchner, G. L. Sun, C. T. Lin, J. T. Park *et al.*, *Phys. Rev. Lett.* **102**, 187005 (2009).
- ¹²J. T. Park, D. S. Inosov, C. Niedermayer, G. L. Sun, D. Haug, N. B. Christensen, R. Dinnebie, A. V. Boris, A. J. Drew, L. Schulz *et al.*, *Phys. Rev. Lett.* **102**, 117006 (2009).
- ¹³S. Sanna, R. De Renzi, G. Lamura, C. Ferdeghini, A. Palenzona, M. Putti, M. Tropeano, and T. Shiroka, *Phys. Rev. B* **80**, 052503 (2009).
- ¹⁴A. D. Christianson, M. D. Lumsden, S. E. Nagler, G. J. MacDougall, M. A. McGuire, A. S. Sefat, R. Jin, B. C. Sales, and D. Mandrus, *Phys. Rev. Lett.* **103**, 087002 (2009).
- ¹⁵D. K. Pratt, W. Tian, A. Kreyssig, J. L. Zarestky, S. Nandi, N. Ni, S. L. Bud'ko, P. C. Canfield, A. I. Goldman, and R. J. McQueeney, *Phys. Rev. Lett.* **103**, 087001 (2009).
- ¹⁶M. Bendele, A. Amato, K. Conder, M. Elender, H. Keller, H.-H. Klauss, H. Luetkens, E. Pomjakushina, A. Raselli, and R. Khasanov, *Phys. Rev. Lett.* **104**, 087003 (2010).
- ¹⁷S. Margadonna, Y. Takabayashi, Y. Ohishi, Y. Mizuguchi, Y. Takano, T. Kagayama, T. Nakagawa, M. Takata, and K. Prassides, *Phys. Rev. B* **80**, 064506 (2009).
- ¹⁸R. Hu, K. Cho, H. Kim, H. Hodovanets, W. E. Straszheim, M. A. Tanatar, R. Prozorov, S. L. Bud'ko, and P. C. Canfield, *Supercond. Sci. Technol.* **24**, 065006 (2011).
- ¹⁹D. H. Ryan, W. N. Rowan-Weetaluktuk, J. M. Cadogan, R. Hu, W. E. Straszheim, S. L. Bud'ko, and P. C. Canfield, *Phys. Rev. B* **83**, 104526 (2011).
- ²⁰W. Bao *et al.*, e-print arXiv:1102.3674.
- ²¹F. Han *et al.*, e-print arXiv:1103.1347.
- ²²B. Shen, B. Zeng, G. F. Chen, J. B. He, D. M. Wang, H. Yang, and H. H. Wen, *EPL* **96**, 37010 (2011).
- ²³Z. Shermadini *et al.* (in preparation).
- ²⁴J. E. Sonier, J. H. Brewer, and R. F. Kiefl, *Rev. Mod. Phys.* **72**, 769 (2000).
- ²⁵E. H. Brandt, *Phys. Rev. B* **68**, 054506 (2003).
- ²⁶J. E. Sonier, W. Huang, C. V. Kaiser, C. Cochran, V. Pacradouni, S. A. Sabok-Sayr, M. D. Lumsden, B. C. Sales, M. A. McGuire, A. S. Sefat *et al.*, *Phys. Rev. Lett.* **106**, 127002 (2011).
- ²⁷The temperature dependence of the superfluid density was analyzed with the fitting package MUSRFIT developed by A. Suter and B. Wojek, [<http://lmu.web.psi.ch/facilities/software/musrfit/user/MUSR/WebHome.html>].
- ²⁸M. Tinkham, *Introduction to Superconductivity* (McGraw-Hill Inc., New York, 1996).
- ²⁹D. A. Torchetti, M. Fu, D. C. Christensen, K. J. Nelson, T. Imai, H. C. Lei, and C. Petrovic, *Phys. Rev. B* **83**, 104508 (2011).
- ³⁰M. I. Tsindlekht, I. Felner, M. Zhang, A. F. Wang, and X. H. Chen, *Phys. Rev. B* **84**, 052503 (2011).
- ³¹S. Bosma, R. Puzniak, A. Krzton-Maziopa, M. Bendele, E. Pomjakushina, K. Conder, H. Keller, and S. Weyeneth, *Phys. Rev. B* **85**, 064509 (2012).
- ³²Y. Zhang, L. X. Yang, M. Xu, Z. R. Ye, F. Chen, C. He, H. C. Xu, J. Jiang, B. P. Xie, J. J. Ying *et al.*, *Nature Mater.* **273**, 10 (2011).
- ³³E. D. Mun, M. M. Altarawneh, C. H. Mielke, V. S. Zapf, R. Hu, S. L. Bud'ko, and P. C. Canfield, *Phys. Rev. B* **83**, 100514 (2011).
- ³⁴J. J. Ying, X. F. Wang, X. G. Luo, A. F. Wang, M. Zhang, Y. J. Yan, Z. J. Xiang, R. H. Liu, P. Cheng, G. J. Ye *et al.*, *Phys. Rev. B* **83**, 212502 (2011).
- ³⁵V. Tsurkan, J. Deisenhofer, A. Günther, H.-A. Krug von Nidda, S. Widmann, and A. Loidl, *Phys. Rev. B* **84**, 144520 (2011).
- ³⁶B. Zeng, B. Shen, G. F. Chen, J. B. He, D. M. Wang, C. H. Li, and H. H. Wen, *Phys. Rev. B* **83**, 144511 (2011).
- ³⁷A. M. Zhang, J. H. Xiao, Y. S. Li, J. B. He, D. M. Wang, G. F. Chen, B. Normand, Q. M. Zhang, and T. Xiang, e-print arXiv:1106.2706.
- ³⁸J. T. Park, G. Friemel, Y. Li, J.-H. Kim, V. Tsurkan, J. Deisenhofer, H.-A. Krug von Nidda, A. Loidl, A. Ivanov, B. Keimer *et al.*, *Phys. Rev. Lett.* **107**, 177005 (2011).
- ³⁹Z. Wang, Y. J. Song, H. L. Shi, Z. W. Wang, Z. Chen, H. F. Tian, G. F. Chen, J. G. Guo, H. X. Yang, and J. Q. Li, *Phys. Rev. B* **83**, 140505 (2011).
- ⁴⁰A. Ricci, N. Poccia, G. Campi, B. Joseph, G. Arrighetti, L. Barba, M. Reynolds, M. Burghammer, H. Takeya, Y. Mizuguchi *et al.*, *Phys. Rev. B* **84**, 060511 (2011).
- ⁴¹P. Cai, C. Ye, W. Ruan, X. Zhou, A. Wang, M. Zhang, X. Chen, and Y. Wang, e-print arXiv:1108.2798.
- ⁴²R. H. Yuan, T. Dong, Y. J. Song, P. Zheng, G. F. Chen, J. P. Hu, J. Q. Li, and N. L. Wang, *Sci. Rep.* **2**, 221 (2011).
- ⁴³A. Charnukha *et al.*, e-print arXiv:1108.5698.
- ⁴⁴V. Ksenofontov, G. Wortmann, S. A. Medvedev, V. Tsurkan, J. Deisenhofer, A. Loidl, and C. Felser, *Phys. Rev. B* **84**, 180508 (2011).
- ⁴⁵I. Nowik, I. Felner, M. Zhang, A. F. Wang, and X. H. Chen, *Supercond. Sci. Technol.* **24**, 095015 (2011).